Adaptive Kalman Filtering based on Matched Filtering of the Innovations Sequence

Wolfgang Niehsen
Robert Bosch GmbH
Corporate Research and Development
D-31132 Hildesheim
Germany
Wolfgang.Niehsen@bosch.com

Abstract – *An adaptive tracking filter for maneuvering targets is developed. The approach is based on matched filtering of the innovations sequence. Analytical solutions based on the invariant subspace method for time-invariant kinematic models along with the corresponding steady-state Kalman filter kernels are derived. Asymptotic and finite-memory operating characteristics are deduced. The proposed adaptive tracking filter is compared to the interacting multiple model filter based on simulation results.*

Keywords: Adaptive Kalman filtering, matched filtering, innovations sequence, invariant subspace method, maneuvering targets

1 Introduction

Tracking of maneuvering targets requires adaptive estimation techniques since the corresponding system models are partially unknown and possibly time varying. Numerous techniques have been developed to deal with this estimation problem containing both stochastic uncertainties and unknown deterministic inputs [1]. These methods can be categorized into four types of approaches, i.e., single filter reactive adaption, variable dimension filtering, cascaded filtering, and multiple model filtering [2]. Adaptive target tracking algorithms often exploit the properties of the zero-mean white-noise innovations sequence. The single filter reactive adaption approach employs the innovations sequence for maneuver detection and reactive filter parameter adjustment. In the case of multiple model filtering [1], [3], [4] and also interacting multiple model filtering [1], [5], the mode likelihood functions are determined by the innovations probability density function (pdf) of mode-matched filters.

In the sequel, an approach to adaptive Kalman filtering based on matched filtering of the innovations sequence will be presented. The approach provides a general maneuver detection method which can be combined with several existing adaptive target tracking algorithms. Analytical solutions are derived for time-invariant kinematic models along with the corresponding steady-state Kalman filter kernels. Furthermore, finite-memory and asymptotic operation characteristics of the proposed adaptive tracking algorithm are deduced.

2 State-space representation

The state-space representation

$$\boldsymbol{x}_{k+1} = \boldsymbol{A}\boldsymbol{x}_k + \boldsymbol{b}u_k + \boldsymbol{g}w_k \ , \tag{1}$$

$$\boldsymbol{y}_k = \boldsymbol{H}\boldsymbol{x}_k + \boldsymbol{v}_k \ , \tag{2}$$

of a general discrete-time dynamic system with state vector $\boldsymbol{x}_k \in \mathbb{R}^N$, deterministic input u_k, system noise w_k, measurement vector $\boldsymbol{y}_k \in \mathbb{R}^M$, and measurement noise $\boldsymbol{v}_k$ will be considered. The matrices $\boldsymbol{A} \in \mathbb{R}^{N\times N}$, $\boldsymbol{H} \in \mathbb{R}^{M\times N}$ and vectors $\boldsymbol{b}, \boldsymbol{g} \in \mathbb{R}^N$ are time-invariant. The zero-mean white-noise processes w_k and $\boldsymbol{v}_k$ are uncorrelated with each other and uncorrelated with the initial state $\boldsymbol{x}_0$, i.e,

$$\mathrm{E}\left[\begin{bmatrix} w_k \\ \boldsymbol{v}_k \\ \boldsymbol{x}_0 \end{bmatrix} [w_l \ \boldsymbol{v}_l \ \boldsymbol{x}_0]\right] = \begin{bmatrix} \sigma_w^2\,\delta_{k,l} & \boldsymbol{O} & \boldsymbol{O} \\ \boldsymbol{O} & \boldsymbol{R}\,\delta_{k,l} & \boldsymbol{O} \\ \boldsymbol{O} & \boldsymbol{O} & \boldsymbol{\Pi}_0 \end{bmatrix} . \tag{3}$$

3 Innovations sequence impulse response

For matched filtering of the innovations sequence

$$\boldsymbol{s}_k := \boldsymbol{y}_k - \boldsymbol{H}\hat{\boldsymbol{x}}_{k|k-1} \tag{4}$$

the impulse response

$$\boldsymbol{h}_k := \boldsymbol{s}_k, \ u_k = \delta_k, \ w_k = 0, \ \boldsymbol{v}_k = 0 \tag{5}$$

has to be determined. With $\boldsymbol{x}_0 = 0$, the state sequence $\boldsymbol{x}_k$ and the measurement sequence $\boldsymbol{y}_k$ can be recursively computed according to (1), (2), i.e.,

$$\boldsymbol{x}_k = \boldsymbol{A}^{k-1}\boldsymbol{b}, \ \boldsymbol{y}_k = \boldsymbol{H}\boldsymbol{A}^{k-1}\boldsymbol{b}, \ k \geq 1 \ . \tag{6}$$

For determination of the predicted state estimate

$$\hat{\boldsymbol{x}}_k := \hat{\boldsymbol{x}}_{k|k-1} \tag{7}$$

we assume that the pair $\{\boldsymbol{A}, \boldsymbol{H}\}$ is completely observable and $\{\boldsymbol{A}, \boldsymbol{Q}^{1/2}\}$ with

$$\boldsymbol{Q} = \boldsymbol{Q}^{1/2}\boldsymbol{Q}^{\mathsf{T}/2} = \sigma_w^2\,\boldsymbol{g}\,\boldsymbol{g}^{\mathsf{T}} \tag{8}$$

is completely controllable, i.e.,

$$\mathrm{rank}\begin{bmatrix} \boldsymbol{H} \\ \boldsymbol{H}\boldsymbol{A} \\ \cdots \\ \boldsymbol{H}\boldsymbol{A}^{N-1} \end{bmatrix} = N \ , \tag{9}$$

$$\mathrm{rank}\left[\boldsymbol{Q}^{1/2} \quad \boldsymbol{A}\boldsymbol{Q}^{1/2} \quad \cdots \quad \boldsymbol{A}^{N-1}\boldsymbol{Q}^{1/2}\right] = N \ . \tag{10}$$

Then, the algebraic Riccati equation

$$\boldsymbol{P} = \boldsymbol{A}\boldsymbol{P}\boldsymbol{A}^\mathsf{T} + \boldsymbol{Q} - \boldsymbol{A}\boldsymbol{P}\boldsymbol{H}^\mathsf{T}(\boldsymbol{H}\boldsymbol{P}\boldsymbol{H}^\mathsf{T} + \boldsymbol{R})^{-1}\boldsymbol{H}\boldsymbol{P}\boldsymbol{A}^\mathsf{T} \quad (11)$$

has a unique positive-definite solution $\boldsymbol{P}$ which determines the innovations covariance matrix

$$\boldsymbol{S} = \boldsymbol{H}\boldsymbol{P}\boldsymbol{H}^\mathsf{T} + \boldsymbol{R} \quad (12)$$

and the steady-state Kalman gain [1]

$$\boldsymbol{K} = \boldsymbol{P}\boldsymbol{H}^\mathsf{T}\boldsymbol{S}^{-1} \; . \quad (13)$$

A nonrecursive algebraic solution for the nonlinear discrete-time Riccati equation (11) can be constructed based on the invariant subspace method [6]. For a nonsingular[1] state transition matrix $\boldsymbol{A}$, (11) can be rewritten as

$$\begin{bmatrix}\boldsymbol{I} & -\boldsymbol{P}\end{bmatrix} \boldsymbol{M} \begin{bmatrix}\boldsymbol{P}\\ \boldsymbol{I}\end{bmatrix} = 0 \; , \quad (14)$$

where

$$\boldsymbol{M} = \begin{bmatrix} \boldsymbol{A}^{-1} & \boldsymbol{A}^{-1}\boldsymbol{Q} \\ -\boldsymbol{H}^\mathsf{T}\boldsymbol{R}^{-1}\boldsymbol{H}\boldsymbol{A}^{-1} & \boldsymbol{A}^\mathsf{T} + \boldsymbol{H}^\mathsf{T}\boldsymbol{R}^{-1}\boldsymbol{H}\boldsymbol{A}^{-1}\boldsymbol{Q} \end{bmatrix} \quad (15)$$

holds. With the above assumption, that $\{\boldsymbol{A}, \boldsymbol{H}\}$ is completely observable and $\{\boldsymbol{A}, \boldsymbol{Q}^{1/2}\}$ is completely controllable, the unique positive-definite solution of (11) is given by

$$\boldsymbol{P} = \boldsymbol{U}\boldsymbol{V}^{-1} \; , \quad (16)$$

where the $N \times N$ matrices $\boldsymbol{U}, \boldsymbol{V}$ form a basis for the stable eigenspace of the $2N \times 2N$ symplectic matrix $\boldsymbol{M}$, i.e.,

$$\boldsymbol{M} \begin{bmatrix}\boldsymbol{U}\\ \boldsymbol{V}\end{bmatrix} = \begin{bmatrix}\boldsymbol{U}\\ \boldsymbol{V}\end{bmatrix} \boldsymbol{\Lambda} \; , \quad (17)$$

where the eigenvalues of the $N \times N$ matrix $\boldsymbol{\Lambda}$ are located strictly inside the unit disc. Note that if λ denotes any eigenvalue of the symplectic matrix $\boldsymbol{M}$, then $1/\lambda^*$ is also an eigenvalue of $\boldsymbol{M}$. Furthermore, $\lambda \neq 0$ and $|\lambda| \neq 1$ hold, so that the spectrum of $\boldsymbol{M}$ contains exactly n nonzero eigenvalues, counting multiplicity, strictly inside the unit disc. Numerical difficulties caused by multiple eigenvalues of $\boldsymbol{M}$ can be solved by Schur triangularization of $\boldsymbol{M}$, i.e.,

$$\begin{bmatrix}\boldsymbol{U}_{11} & \boldsymbol{U}_{12}\\ \boldsymbol{U}_{21} & \boldsymbol{U}_{22}\end{bmatrix}^* \boldsymbol{M} \begin{bmatrix}\boldsymbol{U}_{11} & \boldsymbol{U}_{12}\\ \boldsymbol{U}_{21} & \boldsymbol{U}_{22}\end{bmatrix} = \begin{bmatrix}\boldsymbol{S}_{11} & \boldsymbol{S}_{12}\\ \boldsymbol{O} & \boldsymbol{U}_{22}\end{bmatrix} \; , \quad (18)$$

since $\{\boldsymbol{U}, \boldsymbol{V}\}$ and $\{\boldsymbol{U}_{11}, \boldsymbol{U}_{21}\}$ span the same invariant subspace, so that $\boldsymbol{P} = \boldsymbol{U}_{11}\boldsymbol{U}_{21}^{-1}$ holds. The solution $\boldsymbol{P}$ of the discrete-time Riccati recursion (11) defines the steady-state Kalman gain $\boldsymbol{K}$ according to (13) so that the predicted state estimate $\hat{\boldsymbol{x}}_k$ can be recursively computed as

$$\hat{\boldsymbol{x}}_{k+1} = \boldsymbol{A}_p\hat{\boldsymbol{x}}_k + \boldsymbol{K}_p\boldsymbol{y}_k, \; k \geq 0 \; , \quad (19)$$

where

$$\boldsymbol{A}_p = \boldsymbol{A}(\boldsymbol{I} - \boldsymbol{K}\boldsymbol{H}), \; \boldsymbol{K}_p = \boldsymbol{A}\boldsymbol{K}, \; \hat{\boldsymbol{x}}_0 = 0 \quad (20)$$

holds. The impulse response h_k according to (5) is now completely defined by the measurement sequence $\boldsymbol{y}_k$ (6) and the predicted state estimate $\hat{\boldsymbol{x}}_k$ (19).

[1] The case of singular $\boldsymbol{A}$ can also be solved by the invariant subspace method and leads to a generalized eigenvalue problem [6].

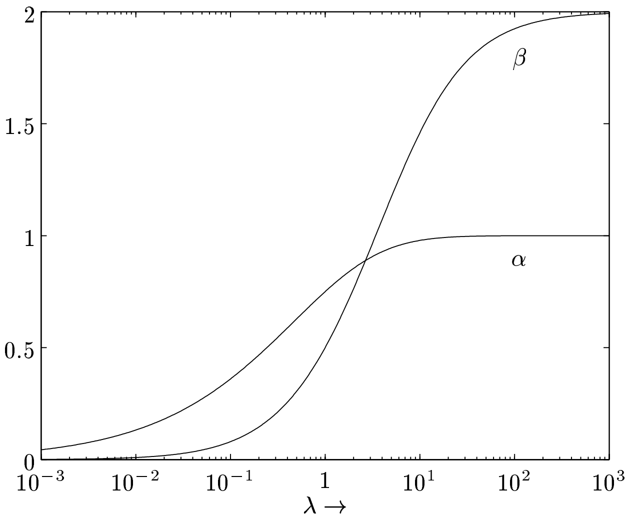

Fig. 1: α-β-filter coefficients for $10^{-3} \leq \lambda \leq 10^3$.

3.1 Second-order kinematic model

The state-space representation (1), (2) of a second-order kinematic model driven by a piecewise constant white-noise acceleration process w_k will be considered, i.e.,

$$\boldsymbol{A} = \begin{bmatrix}1 & T\\ 0 & 1\end{bmatrix}, \; \boldsymbol{b} = \begin{bmatrix}0\\ 1\end{bmatrix} \; , \quad (21)$$

$$\boldsymbol{g} = \begin{bmatrix}\frac{1}{2}T^2\\ T\end{bmatrix}, \; \boldsymbol{H} = \begin{bmatrix}1 & 0\end{bmatrix} \; , \quad (22)$$

$$\boldsymbol{Q} = \mathrm{E}[w_k^2\boldsymbol{g}\boldsymbol{g}^\mathsf{T}] = \sigma_w^2 T^2 \begin{bmatrix}\frac{1}{4}T^2 & \frac{1}{2}T\\ \frac{1}{2}T & 1\end{bmatrix} \; , \quad (23)$$

$$R = \mathrm{E}[v_k^2] = \sigma_v^2 \; . \quad (24)$$

Note that the given choice of $\boldsymbol{b}$ corresponds to a jump u_k of the velocity component of $\boldsymbol{x}_k$. Since analytical solutions for the steady-state Kalman gain and the innovations variance exist, the innovations sequence impulse response (5) can be immediately obtained. With the maneuvering index [1]

$$\lambda = \frac{\sigma_w}{\sigma_v} T^2 \quad (25)$$

the steady-state Kalman gain and the innovations variance are given by

$$\boldsymbol{K} = \begin{bmatrix}\alpha\\ \beta/T\end{bmatrix}, \; \sigma_s^2 = \frac{\sigma_v^2}{1-\alpha} \; , \quad (26)$$

where

$$\alpha = -\frac{1}{8}(\lambda^2 + 8\lambda - (\lambda+4)\sqrt{\lambda^2 + 8\lambda}) \; , \quad (27)$$

$$\beta = \frac{1}{4}(\lambda^2 + 4\lambda - \lambda\sqrt{\lambda^2 + 8\lambda}) \quad (28)$$

holds [1]. Fig. 1 depicts the steady-state Kalman gain coefficients α and β for $10^{-3} \leq \lambda \leq 10^3$. The state and measurement sequences according to (6) are readily obtained:

$$\boldsymbol{x}_k = \boldsymbol{A}^{k-1}\boldsymbol{b} = \begin{bmatrix}(k-1)T\\ 1\end{bmatrix} \; , \quad (29)$$

$$\boldsymbol{y}_k = \boldsymbol{H}\boldsymbol{x}_k = (k-1)T, \; k \geq 1 \; . \quad (30)$$

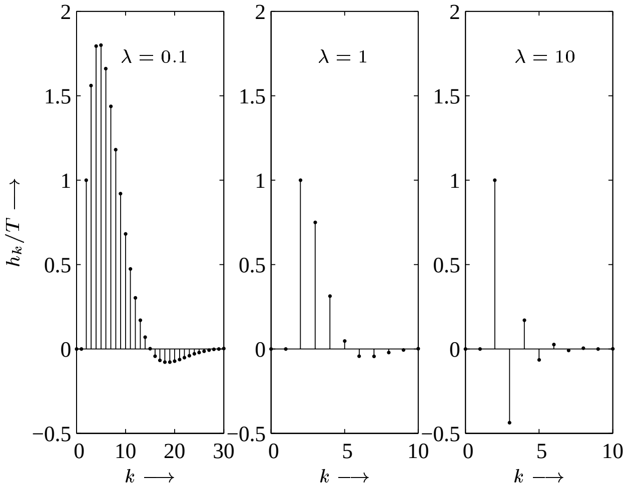

Fig. 2: Innovations sequence impulse response of the α-β-filter for some values of the maneuvering index λ.

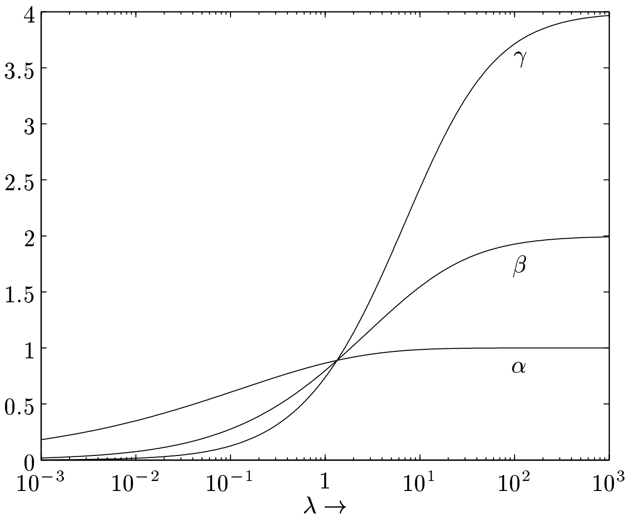

Fig. 3: α-β-γ-filter coefficients for $10^{-3} \leq \lambda \leq 10^{3}$.

The unilateral z-transform of the recursion (19) for the predicted state estimate $\hat{\boldsymbol{X}}(z) = \mathcal{Z}\{\hat{\boldsymbol{x}}_k\}$ leads to

$$\mathcal{Z}\{\hat{\boldsymbol{x}}_k\} = (z\boldsymbol{I} - \boldsymbol{A}_p)^{-1}\boldsymbol{K}_p \mathcal{Z}\{y_k\} \,, \tag{31}$$

where

$$\mathcal{Z}\{y_k\} = \frac{T}{(z-1)^2} \tag{32}$$

holds. Hence, the unilateral z-transform of the innovations sequence impulse response (5) is given by

$$\mathcal{Z}\{h_k\} = \frac{T}{z^2 + z(\alpha+\beta-2) + (1-\alpha)} \,. \tag{33}$$

The partial fraction decomposition

$$\frac{\mathcal{Z}\{h_k\}}{T} = \frac{c_1}{z - z_{\infty,1}} + \frac{c_2}{z - z_{\infty,2}} \tag{34}$$

with the poles of $\mathcal{Z}\{h_k\}$

$$z_\infty = 1 - \frac{\alpha+\beta}{2} \pm \sqrt{\left(\frac{\alpha+\beta}{2}\right)^2 - \beta} \tag{35}$$

and coefficients

$$c_1 = -c_2 = \frac{1}{z_{\infty,1} - z_{\infty,2}} \tag{36}$$

leads to the innovations sequence impulse response

$$\frac{h_k}{T} = \begin{cases} 0, & k = 0 \,, \\ c_1\, z_{\infty,1}^{k-1} + c_2\, z_{\infty,2}^{k-1}, & k \geq 1 \,. \end{cases} \tag{37}$$

Fig. 2 shows h_k/T for some values of the maneuvering index λ. Note that $h_1/T = 0$ and $h_2/T = 1$ holds irrespective of λ.

3.2 Third-order kinematic model

The state-space representation (1), (2) with

$$\boldsymbol{A} = \begin{bmatrix} 1 & T & \frac{1}{2}T^2 \\ 0 & 1 & T \\ 0 & 0 & 1 \end{bmatrix},\ \boldsymbol{b} = \begin{bmatrix} 0 \\ 0 \\ 1 \end{bmatrix} \,, \tag{38}$$

$$\boldsymbol{g} = \begin{bmatrix} \frac{1}{2}T^2 \\ T \\ 1 \end{bmatrix},\ \boldsymbol{H} = \begin{bmatrix} 1 & 0 & 0 \end{bmatrix} \,, \tag{39}$$

$$\boldsymbol{Q} = \mathrm{E}[w_k^2 \boldsymbol{g}\boldsymbol{g}^\mathsf{T}] = \sigma_w^2 \begin{bmatrix} \frac{1}{4}T^4 & \frac{1}{2}T^3 & \frac{1}{2}T^2 \\ \frac{1}{2}T^3 & T^2 & T \\ \frac{1}{2}T^2 & T & 1 \end{bmatrix} \,, \tag{40}$$

$$R = \mathrm{E}[v_k^2] = \sigma_v^2 \,, \tag{41}$$

corresponds to a third-order kinematic model with piecewise constant Wiener process acceleration model. The given choice of $\boldsymbol{b}$ corresponds to a jump u_k of the acceleration component of $\boldsymbol{x}_k$. With the maneuvering index (25) the steady-state Kalman gain and the innovations variance are given by

$$\boldsymbol{K} = \begin{bmatrix} \alpha \\ \beta/T \\ \gamma/(2T^2) \end{bmatrix},\ \sigma_s^2 = \frac{\sigma_v^2}{1-\alpha} \,, \tag{42}$$

where

$$\alpha = 1 - s^2,\ \beta = 2(1-s)^2,\ \gamma = 2\lambda s \tag{43}$$

holds [1]. The parameter s obeys the cubic equation

$$s^3 + (\lambda/2 - 3)s^2 + (\lambda/2 + 3)s - 1 = 0 \tag{44}$$

which can be solved for an appropriate root $0 < s < 1$ by analytical or numerical means. Fig. 3 depicts the steady-state Kalman gain coefficients α, β, γ for $10^{-3} \leq \lambda \leq 10^{3}$. The state and measurement sequences according to (6) are

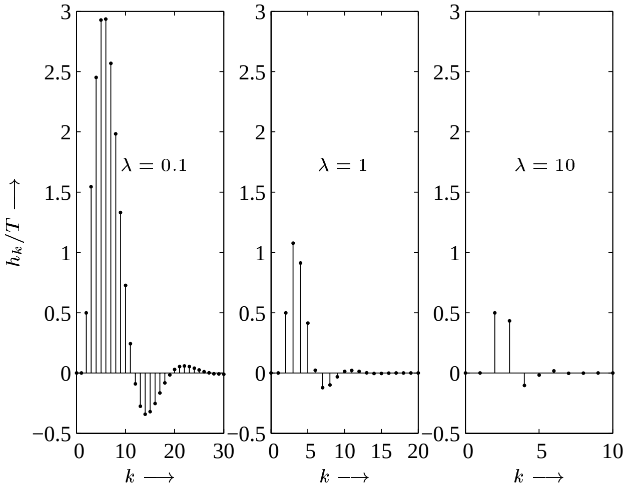

Fig. 4: Innovations sequence impulse response of the α-β-γ-filter for some values of the maneuvering index λ.

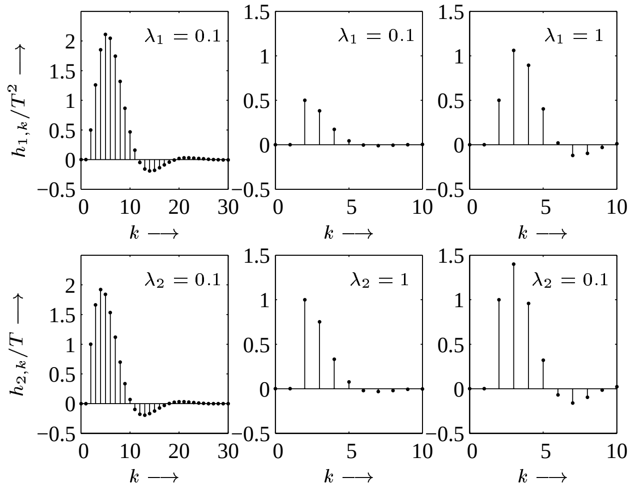

Fig. 5: Innovations sequence impulse response of the steady-state Kalman filter for a third-order kinematic model with position and velocity measurements.

given by

$$\boldsymbol{x}_k = \boldsymbol{A}^{k-1}\boldsymbol{b} = \begin{bmatrix} \frac{1}{2}(k-1)^2T^2 \\ (k-1)T \\ 1 \end{bmatrix} , \tag{45}$$

$$\boldsymbol{y}_k = \boldsymbol{H}\boldsymbol{x}_k = \frac{1}{2}(k-1)^2T^2,\ k \geq 1 \ . \tag{46}$$

With

$$\boldsymbol{A}_p = \begin{bmatrix} 1-(\alpha+\beta+\gamma/4) & T & T^2/2 \\ -(\beta+\gamma/2)/T & 1 & T \\ -\gamma/(2T^2) & 0 & 1 \end{bmatrix} , \tag{47}$$

$$\boldsymbol{K}_p = \begin{bmatrix} \alpha+\beta+\gamma/4 \\ (\beta+\gamma/2)/T \\ \gamma/(2T^2) \end{bmatrix} \tag{48}$$

according to (20), the predicted state estimate (19) and the innovations sequence impulse response (5) can be recursively computed. Fig. 4 shows h_k/T for some values of the maneuvering index λ.

The third-order kinematic model with position and velocity measurements deviates from the state-space representation (38)-(41) with respect to the measurement matrix and the covariance matrix of the measurement noise:

$$\boldsymbol{H} = \begin{bmatrix} 1 & 0 & 0 \\ 0 & 1 & 0 \end{bmatrix} ,\ \boldsymbol{R} = \begin{bmatrix} \sigma_s^2 & 0 \\ 0 & \sigma_v^2 \end{bmatrix} \ . \tag{49}$$

The steady-state Kalman gain $\boldsymbol{K} \in \mathbb{R}^{3\times 2}$ depends only on the maneuvering indices

$$\lambda_1 = \frac{\sigma_w}{\sigma_s}T^2,\ \lambda_2 = \frac{\sigma_w}{\sigma_v}T \tag{50}$$

and can be computed according to the invariant subspace method (12)-(17). The state and measurement sequences are given by

$$\boldsymbol{x}_k = \boldsymbol{A}^{k-1}\boldsymbol{b} = \begin{bmatrix} \frac{1}{2}(k-1)^2T^2 \\ (k-1)T \\ 1 \end{bmatrix} , \tag{51}$$

$$\boldsymbol{y}_k = \boldsymbol{H}\boldsymbol{x}_k = \begin{bmatrix} \frac{1}{2}(k-1)^2T^2 \\ (k-1)T \end{bmatrix} ,\ k \geq 1 \ . \tag{52}$$

With $\boldsymbol{A}_p$ and $\boldsymbol{K}_p$ according to (20), the predicted state estimate $\hat{\boldsymbol{x}}_{k+1}$ and the impulse response

$$\boldsymbol{h}_k = \begin{bmatrix} h_{1,k} \\ h_{2,k} \end{bmatrix} \tag{53}$$

are completely determined. Fig. 5 depicts $h_{1,k}/T^2$ and $h_{2,k}/T$ for several values of the maneuvering indices λ_1, λ_2.

4 Adaptive Kalman filtering

For adaptive Kalman filtering, a likelihood ratio detector for an impulse input $u_k = c\,\delta_{k-k_0}$ can now be constructed as a correlation or matched filter detector which correlates the innovations sequence s_k with a stored replica of the innovations sequence impulse response h_k. Since the impulse response is infinite, the stored replica has to be confined to the range $0 \leq k \leq N_0$. The choice of the matched filter order N_0 is critical since it determines the detector characteristics, i.e., the detection probability P_D and the detection delay. However, these dependencies will be investigated separately, i.e., an upper bound for P_D will be determined for $N_0 \to \infty$ and the degradation for finite N_0 will be considered afterwards.

For a scalar-valued innovations sequence, the correlator output is given by

$$r_k = \sum_{n=k-N_0}^{k} h_{n-k+N_0} s_n \tag{54}$$

with

$$s_n = c\,h_{n-k_0} + e_n \ , \tag{55}$$

where e_n denotes a white-noise process with the innovations variance σ_s^2. Hence,

$$r_k = \sum_{n=k-N_0}^{k} (c\, h_{n-k+N_0} h_{n-k_0} + h_{n-k+N_0} e_n) \quad (56)$$

$$= \sum_{n=0}^{N_0} (c\, h_n h_{n+k-(k_0+N_0)} + h_n e_{n+k-N_0}) \quad (57)$$

$$= c\,\varphi_{k-(k_0+N_0)}^{hh} + \varphi_{k-N_0}^{he} \ , \quad (58)$$

where

$$\varphi_k^{hg} = \sum_{n=0}^{N_0} h_n g_{n+k} \quad (59)$$

holds. Note that φ_k^{hh} denotes a deterministic correlation sequence whereas φ_k^{he} denotes a stationary stochastic process, i.e., a filtered version of e_n. Obviously, the deterministic part of r_k, i.e., the expected value

$$\mathrm{E}[r_k] = c\,\varphi_{k-(k_0+N_0)}^{hh} \quad (60)$$

assumes its maximum for $k = k_0 + N_0$, i.e.,

$$\mu_r = \mathrm{E}[r_{k_0+N_0}] = c\,E_{N_0} \ , \quad (61)$$

where

$$E_{N_0} = \varphi_0^{hh} = \sum_{n=0}^{N_0} |h_n|^2 \quad (62)$$

holds. The stochastic part, $\varphi_{k_0}^{he}$, has zero mean and variance

$$\sigma_r^2 = \mathrm{E}[(\varphi_{k_0}^{he})^2] = \sigma_s^2 E_{N_0}. \quad (63)$$

The unknown deterministic input $u_k = c\,\delta_{k-k_0}$ leads to the hypotheses

$$H_0 : c = 0 \ , \quad (64)$$

$$H_1 : c \neq 0 \ . \quad (65)$$

The corresponding likelihood ratio is given by

$$\Lambda(r) = \frac{p(r|H_1)}{p(r|H_0)} \ , \quad (66)$$

where

$$p(r|H_0) = \frac{1}{\sqrt{2\pi\sigma_r^2}} \exp(-\frac{r^2}{2\sigma_r^2}) \ , \quad (67)$$

$$p(r|H_1) = \frac{1}{\sqrt{2\pi\sigma_r^2}} \exp(-\frac{(r-\mu_r)^2}{2\sigma_r^2}) \quad (68)$$

holds. For a given probability of false alarm P_F, the threshold η of the likelihood ratio or Neyman-Pearson test

$$\ln \Lambda(r) = \underset{H_0}{\overset{H_1}{\gtrless}} \ln \eta \quad (69)$$

is determined by

$$P_F = 2 \int_{r_0}^{\infty} p(r|H_0)\, dr \ , \quad (70)$$

where

$$r_0 = \frac{1}{|\mu_r|} (\sigma_r^2 \ln \eta + \frac{1}{2}\mu_r^2) \quad (71)$$

holds [7].

These results for scalar-valued innovations sequences can be immediately generalized for vector-valued innovations sequences. The correlator output for an M-dimensional innovations sequence is given by

$$\boldsymbol{r}_k = \sum_{n=k-N_0}^{k} \begin{bmatrix} h_{1,n-k+N_0} s_{1,n} \\ \cdots \\ h_{M,n-k+N_0} s_{M,n} \end{bmatrix} \quad (72)$$

with

$$s_{m,n} = c\, h_{m,n-k_0} + e_{m,n}, \ (m = 1, 2, ..., M) \ , \quad (73)$$

where $e_{m,n}$ denotes the m-th component of a zero-mean white-noise process with the innovations covariance matrix $\boldsymbol{S}$. Hence,

$$\boldsymbol{r}_k = \sum_{n=k-N_0}^{k} \begin{bmatrix} h_{1,n-k+N_0}(c\, h_{1,n-k_0} + e_{1,n}) \\ \cdots \\ h_{M,n-k+N_0}(c\, h_{M,n-k_0} + e_{M,n}) \end{bmatrix} \quad (74)$$

$$= \sum_{n=0}^{N_0} \begin{bmatrix} h_{1,n}(c\, h_{1,n+k-(k_0+N_0)} + e_{1,n+k-N_0}) \\ \cdots \\ h_{M,n}(c\, h_{M,n+k-(k_0+N_0)} + e_{M,n+k-N_0}) \end{bmatrix} \quad (75)$$

$$= \begin{bmatrix} c\,\varphi_{k-(k_0+N_0)}^{h_1 h_1} + \varphi_{k-N_0}^{h_1 e_1} \\ \cdots \\ c\,\varphi_{k-(k_0+N_0)}^{h_M h_M} + \varphi_{k-N_0}^{h_M e_M} \end{bmatrix} \ , \quad (76)$$

where

$$\varphi_k^{h_m g_m} = \sum_{n=0}^{N_0} h_{m,n} g_{m,n+k}, \ (m = 1, 2, ..., M) \quad (77)$$

holds. The deterministic part of $\boldsymbol{r}_k$ assumes its componentwise maximum for $k = k_0 + N_0$, i.e.,

$$\boldsymbol{\mu}_r = \mathrm{E}[\boldsymbol{r}_{k_0+N_0}] = c \begin{bmatrix} E_{1,N_0} \\ \cdots \\ E_{M,N_0} \end{bmatrix} \ , \quad (78)$$

where

$$E_{m,N_0} = \varphi_0^{h_m h_m} = \sum_{n=0}^{N_0} |h_{m,n}|^2 \quad (79)$$

holds. The stochastic part of the correlator output has zero mean and its covariance matrix

$$\boldsymbol{C}_r = \boldsymbol{E}_{N_0} \circ \boldsymbol{S} \quad (80)$$

is given by the elementwise Hadamard product [8] of the impulse response correlation matrix

$$\boldsymbol{E}_{N_0} = \sum_{n=0}^{N_0} [h_{m,n} h_{m',n}]_{m,m'=1,2,\ldots,M} \quad (81)$$

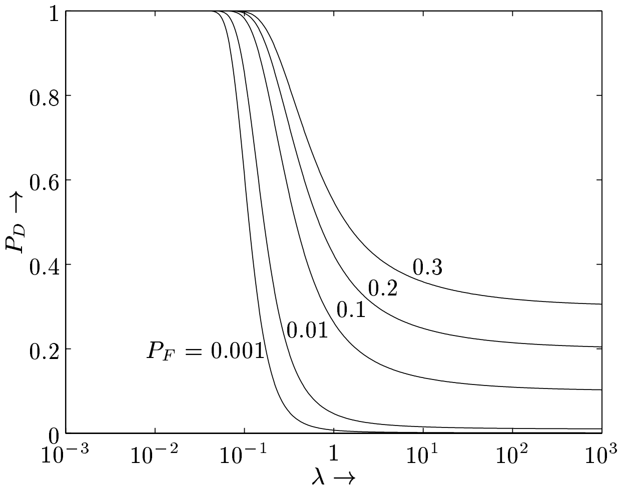

Fig. 6: Receiver operating characteristic of the matched filter detector for the innovations sequence of the α-β-filter for a second-order kinematic model with deterministic input $u_k = c\,\delta_{k-k_0}$. Parameters: $c = 1, \sigma_v = 1, T = 1, N_0 = \infty$.

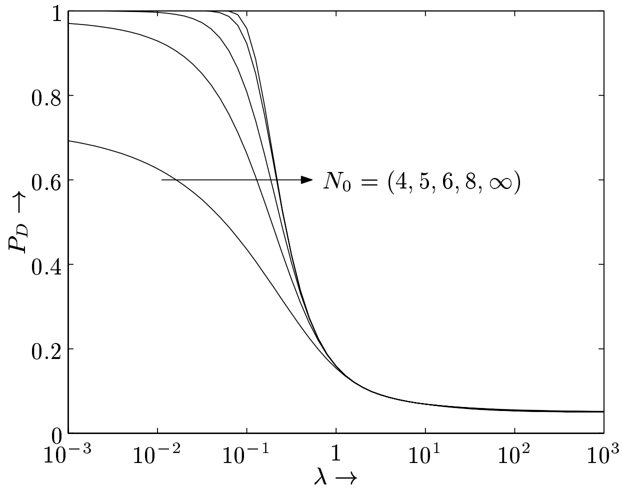

Fig. 7: Receiver operating characteristic of the matched filter detector of order N_0 for the innovations sequence of the α-β-filter for a second-order kinematic model with deterministic input $u_k = c\,\delta_{k-k_0}$. Parameters: $c = 1, \sigma_v = 1, T = 1, P_F = 0.1$.

and the innovations covariance matrix $\boldsymbol{S}$. Thus, the likelihood ratio (66) is completely determined by the multivariate Gaussian pdf's

$$p(r|H_0) = \frac{1}{\sqrt{|2\pi \boldsymbol{C}_r|}} \exp(-\frac{1}{2}\boldsymbol{r}^\mathsf{T}\boldsymbol{C}_r^{-1}\boldsymbol{r}) \;, \tag{82}$$

$$p(r|H_1) = \frac{1}{\sqrt{|2\pi \boldsymbol{C}_r|}} \exp(-\frac{1}{2}(\boldsymbol{r}-\boldsymbol{\mu}_r)^\mathsf{T}\boldsymbol{C}_r^{-1}(\boldsymbol{r}-\boldsymbol{\mu}_r)) \;. \tag{83}$$

For a given probability of false alarm P_F, the threshold η of the likelihood ratio test (69) is determined by [7]

$$P_F = \int_\eta^\infty p(\Lambda|H_1)\, d\Lambda \;. \tag{84}$$

5 Receiver operating characteristics

The receiver operating characteristic of the matched filter detector for the innovations sequence of the α-β-filter with deterministic input $u_k = c\,\delta_{k-k_0}$ and parameters $c = 1, \sigma_v = 1, T = 1, N_0 = \infty$ is shown in Fig. 6. For small maneuvering indices λ the detection probability P_D is close to 1 for all chosen false alarm probabilities P_F. For increasing λ the detection probability P_D decreases and converges asymptotically to P_F since the innovations variance $\sigma_s^2 = \sigma_v^2/(1-\alpha)$ goes to infinity for $\lambda \rightarrow \infty$. The receiver operating characteristics of the matched filter detectors for the innovations sequence of the α-β-filter and the α-β-γ-filter for N_0 finite and $P_F = 0.1$ are depicted in Fig. 7 and Fig. 8, respectively. For small filter orders N_0 the detection probability is significantly lower than in the asymptotic case $N_0 \rightarrow \infty$. However, for sufficiently small maneuver indices $\lambda < 1$, the detection probability P_D is close to 1 even for small matched filter orders N_0.

6 Simulation results

In this section the performance of the proposed matched filter processing of the innovations sequence will be investigated. A maneuvering target with third-order kinematic model according to section 3.2 with $T = 0.1$ and $R = \sigma_v^2 = 1$ is considered. The initial state and the deterministic input are chosen to

$$\boldsymbol{x}_0 = \begin{bmatrix} s_0 & v_0 & a_0 \end{bmatrix}^\mathsf{T} = \begin{bmatrix} 25 & 0 & 0 \end{bmatrix}^\mathsf{T} \tag{85}$$

and

$$u_k = 2\,\delta_{k-20} - 2\,\delta_{k-40} - 4\,\delta_{k-60} + 4\,\delta_{k-70} \;, \tag{86}$$

i.e., the maneuver or nonzero target acceleration intervals are given by

$$a_k = \begin{cases} +2, & 21 \le k \le 40 \;, \\ -4, & 61 \le k \le 70 \;. \end{cases} \tag{87}$$

The matched filter processing of the innovations sequence is employed for adaptive state estimation using $M = 2$ steady-state (α-β-γ) filters with appropriately chosen maneuver indices $\lambda_{1,2}$. The first filter F_1 is chosen to achieve a predetermined stationary position estimation error variance $\sigma_{\hat{s}}^2 = (\frac{1}{4})^2$, i.e., a noise reduction factor of 4:

$$\alpha_1 = \frac{\sigma_{\hat{s}}^2}{\sigma_v^2} = 0.6250 \cdot 10^{-1} \;, \tag{88}$$

$$\beta_1 = 2(2-\alpha_1) - 4\sqrt{1-\alpha_1} = 0.2017 \cdot 10^{-2} \;, \tag{89}$$

$$\gamma_1 = \frac{\beta_1^2}{\alpha_1} = 0.6507 \cdot 10^{-4} \;, \tag{90}$$

$$\lambda_1 = \frac{\gamma_1}{2\sqrt{1-\alpha_1}} = 0.3360 \cdot 10^{-4} \;, \tag{91}$$

$$\sigma_{w_1}^2 = (\frac{\lambda_1 \sigma_v}{T^2})^2 = 0.1129 \cdot 10^{-4} \approx 10^{-5} \;. \tag{92}$$

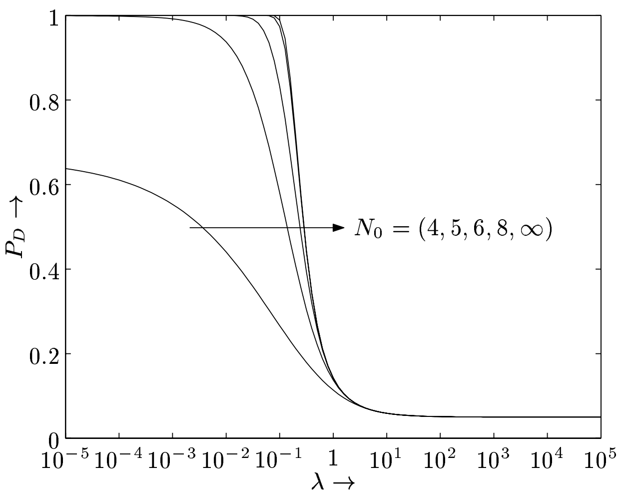

Fig. 8: Receiver operating characteristic of the matched filter detector of order N_0 for the innovations sequence of the α-β-γ-filter for a third-order kinematic model with deterministic input $u_k = c\,\delta_{k-k_0}$. Parameters: $c = 1$, $\sigma_v = 1$, $T = 1$, $P_F = 0.1$.

The process noise of the second filter F_2 is chosen to $\sigma_{w_2} = 10\,\sigma_{w_1}$ in order to achieve a sufficient maneuver tracking performance. Hence, the parameters of the second steady-state filter are given by

$$\sigma_{w_2}^2 = (10\,\sigma_{w_1})^2 = 10^{-3} \,, \tag{93}$$

$$\lambda_2 = \frac{\sigma_{w_2}}{\sigma_v} T^2 = 0.3162 \cdot 10^{-3} \,, \tag{94}$$

$$\alpha_2 = 0.1274 \,, \tag{95}$$

$$\beta_2 = 0.8675 \cdot 10^{-2} \,, \tag{96}$$

$$\gamma_2 = 0.5908 \cdot 10^{-3} \,. \tag{97}$$

A simple multiple model maneuvering target tracking filter can now be constructed based on matched filtering of the innovations sequences of the steady-state filters F_1 and F_2. The multiple model filter is initialized with mode F_1. For mode switching between F_1 and F_2, the innovations sequence is filtered with the corresponding matched filter according to section 3.2 and the likelihood ratio test (69) is employed. The matched filter order N_0 can be determined based on the receiver operating characteristic depicted in Fig. 8. For false alarm probability $P_F = 0.1$, deterministic inputs with $c > 1$, i.e., $a_k > 1$, and maneuver indices $\lambda_1 < \lambda_2 < 10^{-3}$, the detection probability P_D is close to 1 for $N_0 \geq 5$. Hence, for minimum detection delay, the matched filter order is chosen to $N_0 = 5$. The likelihood ratio test threshold $r_0 = 1.645\,\sigma_r$ according to (71) is determined by P_F using equation (70). The variance σ_r^2 of the correlator output is given by $\sigma_r^2 = \sigma_s^2 E_{N_0}$ according to (63).

The proposed adaptive tracking filter is compared to the interacting multiple model (IMM) filter. The Kalman filter kernels of the IMM filter are chosen according the third-order kinematic model of section 3.2 with the same levels of process noise as the steady-state filters $F_{1,2}$. The Markov chain transition matrix is chosen to

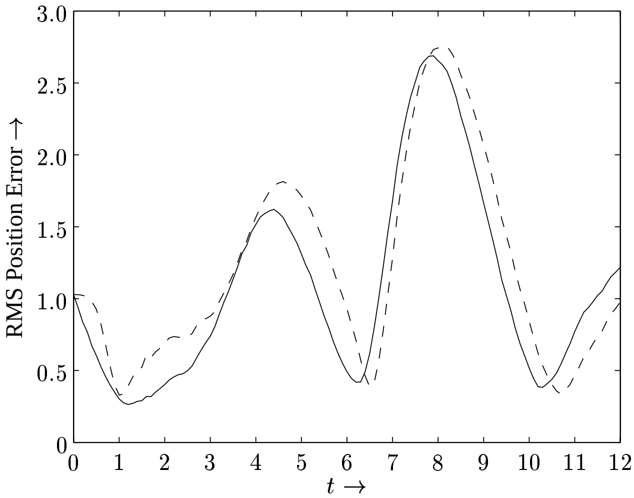

Fig. 9: RMS position errors averaged over 100 runs for the proposed adaptive tracking filter (solid line) and the IMM filter (dashed line) with $M = 2$ models.

$$[p_{ij}] = \begin{bmatrix} 0.95 & 0.05 \\ 0.05 & 0.95 \end{bmatrix} \tag{98}$$

and the initial mode probabilities are chosen to

$$p_1(0) = 0.95,\ p_2(0) = 0.05 \,. \tag{99}$$

The root mean square (RMS) position estimation errors for the proposed adaptive tracking filter and the IMM filter are shown in Fig. 9. The results are averaged over 100 runs. During the nonmaneuvering periods the required noise reduction factor of 4 corresponding to an RMS level of 0.25 is approximately achieved for both adaptive tracking filters. The RMS levels during maneuvering periods are also close to each other. Hence, the performance of the proposed adaptive tracking filter based on matched filtering of the innovations sequence is close to the IMM filter. Moreover, the computational requirements of the proposed adaptive tracking filter are low since steady-state filter kernels are employed and explicit calculations of mode likelihood functions are not required.

7 Summary and conclusions

An adaptive tracking filter for maneuvering targets based on matched filtering of the innovations sequence is developed. The approach provides a general maneuver detection method which can be combined with several existing target tracking algorithms. The innovations sequence impulse response for a general discrete-time dynamic system is constructed based on the invariant subspace method which provides a nonrecursive algebraic solution for the nonlinear discrete-time Riccati equation. Analytical solutions for second-order and third-order kinematic models with position and also position and velocity measurements are derived. For adaptive Kalman filtering, a likelihood ratio detector based on matched filtering of the innovations sequence is developed. The asymptotic and finite-memory receiver operating characteristics are deduced. Simulation results reveal that the performance of the proposed adaptive tracking filter is close to the IMM filter. The computational requirements of the proposed adaptive tracking filter are low since steady-state filter kernels are employed and explicit calculations of mode likelihood functions are not required.

References

[1] Y. Bar-Shalom and X. R. Li. *Estimation and Tracking*. Norwood, MA: Artech House, 1993.

[2] S. Blackmann and R. Popoli. *Modern Tracking Systems*. Norwood, MA: Artech House, 1999.

[3] X.-R. Li and Y. Bar-Shalom. Multiple-model estimation with variable structure. *IEEE Trans. Automat. Contr.*, 41(4):478–493, April 1996.

[4] P. D. Hanlon and P. S. Maybeck. Multiple-model adaptive estimation using a residual correlation Kalman filter bank. *IEEE Trans. Aerospace and Electronic Syst.*, 36(2):393–406, April 2000.

[5] H. A. P. Blom and Y. Bar-Shalom. The interacting multiple model algorithm for systems with Markovian switching coefficients. *IEEE Trans. Aerospace and Electronic Syst.*, 33(8):780–783, August 1988.

[6] T. Kailath, A.H. Sayed, and B. Hassibi. *Linear Estimation*. Englewood Cliffs, NJ: Prentice Hall, 2000.

[7] L. L. Scharf. *Statistical Signal Processing: Detection, Estimation, and Time Series Analysis*. Reading, MA: Addison-Wesley, 1990.

[8] R. A. Horn and C. R. Johnson. *Topics in Matrix Analysis*. Cambridge University Press, 1995.